

# Synthesis and properties of segmented copolymers having aramid units of uniform length

M.C.E.J. Niesten, J. Feijen, R.J. Gaymans\*

University of Twente, P.O. Box 217, 7500 AE Enschede, The Netherlands

Received 20 February 2000; accepted 29 March 2000

## Abstract

Segmented copolymers consisting of crystallizable *p*-phenyleneterephthalamide ester units and poly(tetramethyleneoxide) segments were synthesized. The synthesis of the *p*-phenyleneterephthalamide ester starting material was optimized with respect to yield and purity. The polymers were synthesized via a solution/melt polymerization. The possibilities for a melt polymerization are also discussed. The length of the poly(tetramethyleneoxide) segment in the polymers was varied from 650 to 2900 g/mol. Also other types of low  $T_g$  segments were incorporated in the polymers: modified poly(tetramethyleneoxide) (methyl side groups), poly(oxyethyleneglycol) and poly(ethylene/butylene). The polymer properties were investigated with differential scanning calorimetry (DSC) and dynamic mechanical analysis (DMA). The polymers are fast crystallizing and the *p*-phenyleneterephthalamide units crystallize nearly completely. As a result the glass transition is sharp and low ( $-65^\circ\text{C}$ ), the rubbery plateau is temperature independent and the flow temperature is high. Polymers with poly(oxyethyleneglycol) have a high water uptake. Polymers with poly(ethylene/butylene) segments already phase separate during the polymerization inhibiting the formation of high molecular weight polymers. © 2000 Elsevier Science Ltd. All rights reserved.

**Keywords:** Segmented copolymers; Copolyetheresteramides; Bisesterdiamides

## 1. Introduction

In general, segmented copolymers consist of alternating hard and soft segments. The hard segments crystallize in lamellae and form physical crosslinks for the amorphous (soft) segments. Some of the hard segments do not crystallize and are present in the amorphous phase. If they are miscible with the soft segments, one glass transition temperature ( $T_g$ ) is found and  $T_g$  increases with the hard segment content in the amorphous phase. This morphology accounts for the typical thermoplastic elastomer behavior [1,2].

Segmented copolymers are often made via polycondensation reactions resulting in polydisperse materials. Especially the polydispersity of the hard segments influences the thermal and mechanical properties of the polymers. Harrell [3], Ng et al. [4] and Eisenbach [5] investigated both the behavior of uniform and non-uniform hard segments in non-hydrogen bonding polyurethanes. It was concluded that hard segments of uniform length crystallize faster and better than hard segments of non-uniform length. If the non-crystallized hard segments are poorly miscible with the amorphous soft segments, hardly any hard segments will

be present in the amorphous phase resulting in a low glass transition temperature ( $T_g$ ) and high melting temperature ( $T_m$ ) [2].

Harrell [3] observed a higher strain at break for polymers with uniform non-hydrogen bonding urethane segments than for similar polymers with non-uniform urethane segments. In accordance with this observation, Miller et al. [6] found a higher strain for segmented copolymers with a narrow length distribution of the hard and soft segments than for polymers with broad segment length distributions.

Kirikihiro et al. [7] synthesized segmented copolymers with crystallizable uniform aramid segments and poly(tetramethyleneoxide), PTMO, soft segments. The rubbery plateau of these polymers was temperature independent.

Hirt and Herlinger [8] studied alternating poly(etheresteramide)s with uniform aromatic amide segments and alkanediols or PTMO soft segments. They found that in order to obtain a continuous polyether phase, the minimal molecular weight of the PTMO segment should be 650 g/mol.

Gaymans [9] and Van Hutten [10] described the synthesis of segmented copolymers with bisesterdiamide units of uniform length. These polymers were synthesized from 1,4-butylene terephthalamide (T4T-dimethyl) and aliphatic diols or PTMO. The T4T units crystallized very fast and

\* Corresponding author.

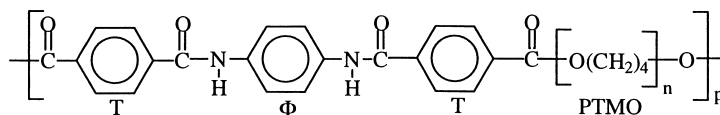


Fig. 1. Structure of segmented copolymer TΦT-PTMO.

nearly completely resulting in a low diamide concentration in the polyether phase. With increasing soft segment length, the  $T_m$  decreased from 185°C (PTMO<sub>250</sub>) to 84°C (PTMO<sub>2900</sub>) which was ascribed to the solvent effect described by Flory [11]. The uniform T4T segments form perfect and stable crystalline lamellae, resulting in a temperature independent rubbery plateau. With increasing PTMO length, the stress-strain curves more and more resembled those of typical elastomers, showing a low initial modulus, a sigmoidal curve and a strain at break exceeding 1000%. T4T-PTMO copolymers possess a very nice combination of properties, which makes them interesting as thermoplastic elastomers. A disadvantage is, however, their low melting temperature. In order to obtain copolymers with a higher melting temperature 1,4-phenyleneterephthalamide (TΦT) was used instead of T4T (Fig. 1).

So far, little research on the synthesis and properties of segmented copolymers with uniform crystallizable aramid units has been carried out. Segmented copolymers based on TΦT hard segments and polyether soft segments are expected to possess excellent thermoplastic elastomer properties, such as a low  $T_g$ , a high  $T_m$ , but still low enough to allow melt processing and a temperature independent rubbery plateau.

### 1.1. Synthesis of copolyetheresteramides with uniform amide segments

Segmented copolyetheresteramides with uniform amide segments can be easily prepared from the preformed bisesterdiamides as the starting compounds [7,9,12,13]. Via a polycondensation with hydroxyl functionalized soft segments in the presence of an esterification catalyst such as tetraisopropyl orthotitanate the bisesterdiamides are then further reacted to form segmented copolymers. In this way, the uniformity of the hard segments is maintained. The synthesis of fully aromatic bisesterdiamides has been reported previously [7,13–18].

It would be interesting to find a way to make copolyetheresteramides with uniform amide segments without having to synthesize the high melting bisesterdiamide first. An option could be to first synthesize PTMO segments with terephthalic acid, terephthalic acid chloride or phenyl terephthalate end groups. By subsequent reaction with an aromatic diisocyanate or an aromatic diamine, polymers with uniform amide segments could be formed. Kirikihira et al. [7] reports a one-pot solution polymerization of PTMO with butyl 4-aminobenzoate (step 1) and terephthaloyl chloride (step 2). Uniform amide segments were formed since terephthaloyl

chloride was added after most of the PTMO was end-capped with aminobenzoate. Direct esterification in the bulk of PTMO with terephthalic acid is used for the formation of segmented copolyetheresters with poly(butylene terephthalate) or poly(ethylene terephthalate) hard segments and PTMO soft segments [19,20]. Terephthalic acid dissolves in the PTMO/butanediol or PTMO/ethanediol mixture. Imai et al. [21] reported the direct polycondensation of aromatic diamines and aromatic diacids in the presence of triphenyl phosphate and pyridine in an NMP solution to form polyether-aramid multi-block copolymers. Ueda et al. [22] studied the polycondensation of diphenyl terephthalate with bis(4-aminophenyl)ether to form the corresponding aromatic polyamide. The reaction was catalyzed by 1-hydroxybenzotriazole and carried out at 70°C for five days, NMP being used as the solvent. The molecular weights obtained were quite low. Aromatic diisocyanates react with dicarboxylic acids to form aromatic polyesteramides in the presence of phospholene-oxides as the catalyst [23–26].

In this study, the syntheses and properties of TΦT-PTMO copolymers are investigated. Firstly, the solution/melt polymerization from the preformed TΦT-dimethyl and PTMO and the melt polymerization from TΦT-didecanyl with PTMO is presented. Secondly, possibilities for a solvent free, one-pot polymerization will be discussed. Thirdly, the influence of the PTMO length on the polymer properties is studied. Finally, different amorphous segments (PTMO, modified PTMO (PTMO<sub>m</sub>), poly(oxyethylene-glycol) (PEG) and poly(ethylene/butylene) at (PEB) will be incorporated in the polymers and the properties will be compared.

## 2. Experimental

### 2.1. Materials

Dimethyl terephthalate (DMT), terephthaloyl chloride (TPC), phenol, terephthalic acid (TPA), *p*-phenylenediamine (PPA), poly(oxyethylene-glycol) (PEG,  $M = 1000$  g/mol) anhydrous methanol, anhydrous toluene, sodium methanolate and *N*-methyl-2-pyrrolidone (NMP) were purchased from Merck. Tetraisopropyl orthotitanate ( $Ti(i-OC_3H_7)_4$ ), obtained from Merck, was diluted in anhydrous *m*-xylene (0.05 M), obtained from Fluka. Methyl(4-chlorocarbonyl)benzoate (MCCB) was obtained from Dalian (No. 2 Organic Chemical Works, China). Poly(tetramethyleneoxide) ((PTMO,  $M = 650$ –2900 g/mol)

was provided by DuPont and modified PTMO (PTMOM, PTMO containing 15 wt% of methyl side groups,  $M = 1000\text{--}3000$  g/mol) was obtained from Mitsui (PTG-L). Hydroxyl functionalized Poly(ethylene/polybutylene) (PEB,  $M = 3300$  g/mol) was provided by Shell (Kraton liquid polymer L-2203). Irganox 1330 was obtained from CIBA. All chemicals were used as received.

## 2.2. Synthesis of T $\Phi$ T-dimethyl

The CA index name of T $\Phi$ T-dimethyl is benzoic acid, 4,4'-[1,4-phenylenebis(iminocarbonyl)]bis-, dimethyl ester, no. 56419-58-0.

### 2.2.1. Route I

TPC (100 g, 0.5 mol) was dissolved in 1 l NMP at room temperature in a 2 l flask, equipped with a mechanical stirrer, a nitrogen inlet, a condenser and a calcium chloride tube. PPA (15 g, 0.14 mol), previously dissolved in 200 ml NMP, was added dropwise over a period of 30 min, and methanol (250 ml) was added after 90 min reaction time. Subsequently, the temperature was raised to 160°C. After stirring for 15 min, the reaction mixture was filtered through paper filters and the filtrate was left to cool overnight. The precipitated product was filtered through a glass filter (pore size 4) and washed in hot toluene, and twice with hot acetone. The product was subsequently dried in a vacuum oven at 70°C.

### 2.2.2. Route II

MCCB (61 g, 0.31 mol) was dissolved in 400 ml NMP at room temperature in a 1 l flask, equipped with mechanical stirrer, nitrogen inlet, condenser and calcium chloride tube. PPA (15 g, 0.14 mol), previously dissolved in 200 ml NMP, was added dropwise over a period of 30 min, and methanol (50 ml) was added after a 2 hour reaction time. After 2 h, the reaction mixture was filtered off in a soxhlet extraction thimble and washed with hot toluene, and twice in hot acetone. The product was subsequently dried in a vacuum oven at 70°C.

## 2.3. Synthesis of T $\Phi$ T-didecanyl

TPC (100 g, 0.5 mol) was dissolved at room temperature in 400 ml NMP in a 2 l flask equipped with a mechanical stirrer, a condenser, a calcium chloride tube and a nitrogen inlet. PPA (15 g, 0.14 mol), previously dissolved in 400 ml NMP, was added dropwise to the reaction over a period of 30 min and decanol (250 ml) was added after 3 h reaction time. The temperature was raised to 75°C and the reaction was continued for 4 h. The reaction mixture was poured into a soxhlet extraction thimble, the product was washed twice in hot toluene and dried in a vacuum oven at 70°C overnight. The T $\Phi$ T-didecanyl obtained was further purified by recrystallization from NMP (125°C, 30 g/l) and washed twice in hot acetone and again dried in a vacuum oven at 70°C overnight.

## 2.4. Synthesis of diphenyl terephthalate (DPT)

TPC (25 g, 0.12 mol) was dissolved at room temperature in 100 ml NMP in a 500 ml flask equipped with a magnetic stirrer, a condenser, a calcium chloride tube and a nitrogen inlet. Phenol (50 g, 0.54 mol), previously dissolved in a 100 ml NMP was added. The reaction was carried out for 16 h. Water was added to precipitate the product. The precipitate was filtered off through a glass filter (pore size 4) and washed in ethanol twice. The product was subsequently dried in a vacuum oven at 70°C.

## 2.5. Reaction between DPT and PPA

The reaction was carried out in a 250 ml vessel with a nitrogen inlet and a mechanical stirrer. The vessel containing DPT (5 g, 15.7 mmol), PPA (3.4 mmol), 100 ml NMP and sodium methanolate (0.085 g, 1.57 mmol) was heated to 200°C and left for 2 h. The vessel was then cooled and the product was precipitated with diethylether. The precipitate was filtered through a glass filter (pore size 4) and dried in a vacuum oven overnight at 70°C.

## 2.6. Polymerization

### 2.6.1. Route I. Solution/melt polymerization starting from T $\Phi$ T-dimethyl

The preparation of T $\Phi$ T-PTMO<sub>1000</sub> is shown as an example. The reaction was carried out in a 250 ml stainless steel vessel with a nitrogen inlet and a mechanical stirrer. The vessel, containing T $\Phi$ T-dimethyl (4.32 g, 0.01 mol), PTMO<sub>1000</sub> (10 g, 0.01 mol), Irganox 1330 (0.2 g), and 100 ml NMP was heated in an oil bath to 180°C, then the catalyst solution was added (1 ml of 0.05 M Ti(*i*-OC<sub>3</sub>H<sub>7</sub>)<sub>4</sub> in *m*-xylene). After 30 min reaction time, the temperature was raised to 250°C and maintained for 2 h. The pressure was then carefully reduced ( $P < 20$  mbar) to distil off NMP and then further reduced ( $P < 1$  mbar) for 60 min. Finally, the vessel was allowed to slowly cool to room temperature whilst maintaining the low pressure. For the other diols (PTMO<sub>m</sub>, PEG<sub>1000</sub> and Kraton<sub>3300</sub>), the same polymerization procedure was followed.

### 2.6.2. Route II. Melt polymerization starting from T $\Phi$ T-didecanyl

T $\Phi$ T-didecanyl (6.84 g, 0.01 mol), PTMO<sub>1000</sub> (10 g, 0.01 mol) and the catalyst solution (1 ml of 0.05 M Ti(*i*-OC<sub>3</sub>H<sub>7</sub>)<sub>4</sub> in *m*-xylene) were mixed and extruded at 275°C in a 4 cc DSM res RD11H-1009025-4 corotating twin screw mini extruder. The hot extrudate was collected in a hot 250 ml stainless steel vessel with a nitrogen inlet and a mechanical stirrer. Again, catalyst solution was added (1 ml of 0.05 M Ti(*i*-OC<sub>3</sub>H<sub>7</sub>)<sub>4</sub>) and the temperature was raised to 250°C and maintained for 2 h. The pressure was then carefully reduced ( $P < 1$  mbar) for 60 min. Finally, the vessel was allowed to slowly cool to room temperature whilst maintaining the low pressure.

### 2.6.3. Route III. Solvent free one-pot polymerization from DPT, PTMO and PPA

The reaction was carried out in a 250 ml vessel with a nitrogen inlet and a mechanical stirrer. The vessel containing PTMO<sub>1000</sub> (30 g, 0.03 mol) and DPT (14.4 g, 0.045 mol), Irganox 1330 (0.3 g) and catalyst solution (3 ml of 0.05 M Ti(*i*-OC<sub>3</sub>H<sub>7</sub>)<sub>4</sub> in *m*-xylene) was heated to 220°C and maintained for 1 h. The temperature was then raised to 250°C and the reaction was carried out for another hour. Finally a low vacuum ( $P < 20$  mbar) was applied for one hour followed by high vacuum ( $P < 1$  mbar) for another hour. After cooling to room temperature, the product was analyzed by <sup>1</sup>H NMR to calculate the PTMO/DPT overall soft segment length (4773 g/mol). Subsequently, a two-fold excess of PPA was added (0.8 g, 7.6 mmol PPA per 20 g (3.8 mmol) of soft segment PTMO<sub>1000</sub>/DPT) and sodium methanolate was added as a catalyst (10.6 mg, 0.2 mmol). The temperature was raised to 220°C and maintained for 45 min. Then the temperature was raised to 250°C and after 60 min a low vacuum ( $P < 20$  mbar) was applied for an hour. The pressure was then reduced further ( $P < 1$  mbar) and left for another hour. Finally, the vessel was allowed to slowly cool to room temperature whilst maintaining the low pressure.

### 2.7. NMR

<sup>1</sup>H NMR spectra were recorded on a Bruker AC 250 spectrometer at 250.1 MHz. For all the samples, except for the TΦT-dimethyl samples, deuterated trifluoroacetic acid (TFA-d) was used as a solvent. Deuterated sulfuric acid (D<sub>2</sub>SO<sub>4</sub>) was used as the solvent for TΦT-dimethyl.

### 2.8. GPC

GPC measurements were carried out with polymer solutions in *m*-cresol (5 mg/l), filtrated via 0.45 μm Schleicher and Schuell filters. The molecular weight was determined using a Waters model 150C ALC/GPC with two HT 6E Styrogel columns and refractive index (RI) detection, using a 0.6 ml/min flow of *m*-cresol at 70°C. Calibration was performed with 10 nearly monodisperse polystyrene standards (range 330,000–1920).

### 2.9. DSC

DSC spectra were recorded on a Perkin–Elmer DSC7 apparatus, equipped with a PE7700 computer and TAS-7 software. Dried sample (2–5 mg) was heated at a rate of 20°C/min. For TΦT-dimethyl, the onset of the melting peak of the first heating scan was used as the melting temperature, the peak area was used to calculate the melt enthalpy. For the polymers, first cooling and second heating scan was used to determine the melting and crystallization peaks. The peak maximum or minimum was used as the melting or crystallization temperature, respectively, the peak area as the enthalpy.

### 2.10. Viscometry

The inherent viscosity of the polymers at a concentration of 0.1 g/dl in a 1:1 (molar ratio) mixture of phenol/1,1,2,2-tetrachloroethane at 25°C, was determined using a capillary Ubbelohde 1B.

### 2.11. DMA

Samples for the DMA test (70 × 9 × 2 mm<sub>3</sub>) were prepared on an Arburg H manual injection molding machine. The barrel temperature of the injection molding machine was set at 50°C above the melting temperature of the polymer, with the temperature being held at room temperature.

Using a Myrenne ATM3 torsion pendulum at a frequency of approximately 1 Hz the values of the storage modulus  $G'$  and the loss modulus  $G''$  as a function of the temperature were measured. Dried samples were first cooled to –100°C and then subsequently heated at a rate of 1°C/min with the maximum of the loss modulus being taken as the glass transition temperature. The flow temperature was defined as the temperature where the storage modulus reached 1 MPa.

### 2.12. Water absorption

The absorption of water was measured as the weight gain after conditioning (see Eq. (1)). DMA test bars were dried at 100°C in a vacuum oven overnight and weighted ( $w_0$ ), the samples were then conditioned in a dessicator over water at room temperature for seven days and then reweighed ( $w$ )

$$\text{water absorption} = \frac{w - w_0}{w_0} \times 100\% \quad (1)$$

## 3. Results and discussion

### 3.1. Introduction

The polymers were synthesized according to three routes: the solution/melt polymerization starting from TΦT-dimethyl, a melt polymerization starting from TΦT-didecanyl and a one-pot melt polymerization starting from diphenyl terephthalate, *p*-phenylenediamine and PTMO. Firstly, the TΦT-dimethyl and TΦT-didecanyl syntheses are described followed by the polymerization. The possibilities for a solvent free, one-pot polymerization are discussed. Polymers with PTMO segments of different lengths were synthesized and the properties are studied. Finally, different types of soft segments were incorporated in the polymers and the polymer properties are compared.

### 3.2. Synthesis of TΦT-dimethyl and TΦT-didecanyl

TΦT-dimethyl was synthesized from terephthaloyl chloride (TPC), *p*-phenylenediamine (PPA) and methanol according to the method described by Mangnus [15] and

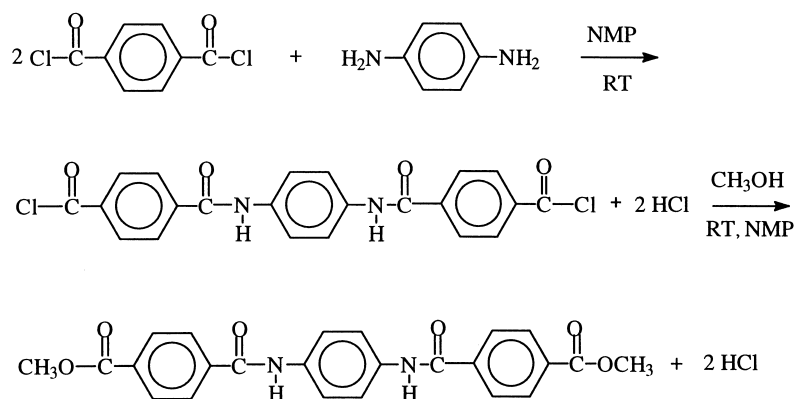


Fig. 2. Reaction scheme for the synthesis of TΦT-dimethyl from terephthaloyl chloride, *p*-phenylenediamine and methanol (route I).

Den Breejen [16] (route I). Acid chloride groups react rapidly with amines to form amides at room temperature, without a catalyst. The reaction scheme is given in Fig. 2. An excess (2.2) of TPC was reacted with PPA at room temperature in an NMP solution. NMP also functions as an acid scavenger for the HCl that was formed during the reaction. The acid chloride end-groups of the intermediate product were reacted with methanol. In this way TΦT-dimethyl was formed and it precipitated from the reaction mixture. The reaction between TPC and PPA is very fast and the build up of higher oligomers such as TΦTΦT-dimethyl cannot be avoided. Also some half product (TΦ) might have been formed. The side products were removed from pure TΦT-dimethyl by recrystallization from NMP. Since NMP was already the reaction solvent, the recrystallization step was carried out directly after the synthesis in the original reaction flask. The reaction mixture was heated to 160°C. At this temperature TΦ and TΦT-dimethyl are expected to dissolve, while the higher oligomers are expected to remain insoluble. The higher oligomers were filtered off. After cooling down to room temperature, TΦT-dimethyl precipitated while TΦ remained in solution.

The purity of TΦT-dimethyl is very important as it affects the uniformity of the aramid segments in the polymers. The purity of TΦT-dimethyl was checked with  $^1\text{H}$  NMR. In Fig. 3, the aromatic region of the  $^1\text{H}$  NMR spectrum of crude and recrystallized TΦT-dimethyl are given. The peak assignment is also shown in Fig. 3 and the chemical shifts in Table 1. An estimation of the purity of TΦT-dimethyl was obtained using Eq. (2)

$$\text{purity} = \left(2 - \frac{b}{c}\right) \times 100\% \quad (2)$$

In which *b* and *c* are the integrals of the corresponding peaks. If higher oligomers such as TΦTΦT-dimethyl are present the integral of peak *b* increases. If TΦ is present peak *c'* appears. The small peak downfield to peak *a* of the crude product belongs to dimethyl terephthalate. The excess of the TPC has reacted with methanol to form dimethyl terephthalate. After recrystallization this peak disappeared. The results of the TΦT-dimethyl syntheses, together with the results of the TΦT-didecanyl syntheses are given in Table 2. TΦT-didecanyl was synthesized according to the

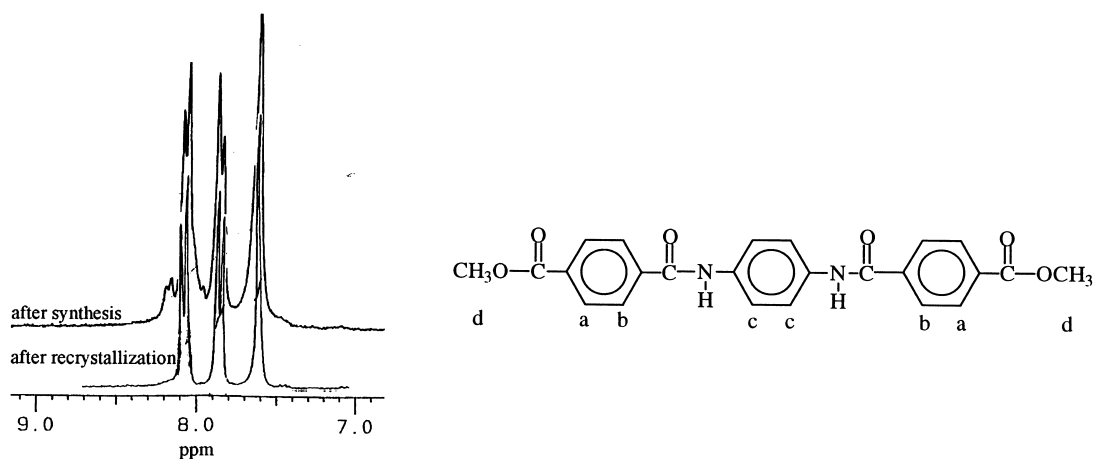


Fig. 3.  $^1\text{H}$  NMR scan of aromatic peaks of TΦT-dimethyl after synthesis and after recrystallization from NMP.

Table 1  
Chemical shifts  $\delta$  of protons of T $\Phi$ T-dimethyl

Peak	Chemical shift $\delta$ (ppm)	Type	Description	Integral
a	8.0–8.1	Doublet	Terephthalic H, ester side	1
b	7.8–7.9	Doublet	Terephthalic H, amide side	1
c	7.6	Singlet	Aromatic PPA H, in T $\Phi$ T-dimethyl	1
c'	7.5	Singlet	Free aromatic PPA H	0
d	4.3	Singlet	CH <sub>3</sub> peak	1.5

method described above whereby methanol was replaced by decanol.

The purity of the formed T $\Phi$ T-dimethyl and T $\Phi$ T-didecanyl is always high (>95%, within the error of NMR). The DSC melting peaks are always sharp, also an indication that the products are pure. T $\Phi$ T-dimethyl has a very high melting temperature of 371°C and consequently, the use of a solvent for polymerization cannot be avoided. The melting temperature is lowered with 100°C when decanyl ester end groups are used instead of methyl end groups. The yield of both reactions is rather low, lower than 20% for T $\Phi$ T-dimethyl and lower than 40% for T $\Phi$ T-didecanyl due to the formation of the side products.

The formation of higher oligomers such as T $\Phi$ T $\Phi$ T-dimethyl can be avoided and thus the yield increased by synthesizing T $\Phi$ T-dimethyl from the mono acid chloride of terephthalic acid, methyl(4-chlorocarbonyl)benzoate (MCCB) (route II). MCCB was reacted with *p*-phenylenediamine in an NMP solution. The reaction scheme is given in Fig. 4. NMP also functions as an acid scavenger for HCl. Pure T $\Phi$ T-dimethyl was formed very easily since no side reactions occurred. The purity of the product obtained in this way is high (>95%) and the DSC melting peaks are sharp. The yield of this reaction is always higher than 90%, making this a very interesting route to synthesize T $\Phi$ T-dimethyl. A disadvantage is the availability of MCCB. T $\Phi$ T-dimethyl is used for a solution/melt polymerization, T $\Phi$ T-didecanyl is used in a melt polymerization as will be discussed in the next paragraph.

### 3.3. Solution/melt polymerization of T $\Phi$ T–PTMO (route I)

T $\Phi$ T-dimethyl is polymerized with hydroxyl functionalized PTMO in a two step synthesis. The polymerization

Table 2  
Results of T $\Phi$ T-dimethyl and T $\Phi$ T-didecanyl syntheses

Compound	Yield <sup>a</sup> (%)	Purity <sup>b</sup> (%)	$T_m$ (°C)	$\Delta H_m$ (J/g)
T $\Phi$ T-dimethyl	15	96	371	234
	20	98	372	240
T $\Phi$ T-didecanyl	32	95	274	102
	37	98	271	90

<sup>a</sup> After recrystallization.

<sup>b</sup> According to Eq. (2).

route is given in Fig. 5. The polymerization consists of a transesterification followed by a polycondensation, tetraisopropyl orthotitanate being used as the catalyst for both steps. For the transesterification a solvent (NMP) was needed because of the high melting temperature of T $\Phi$ T-dimethyl (371°C), combined with the maximum reaction temperature of 250°C due to thermal instability of PTMO above this temperature [27]. To prevent degradation of PTMO during polymerization and subsequent melt processing, Irganox 1330 was added as a stabilizer (1 wt%). During the transesterification, the methyl ester end groups were transesterified with the hydroxyl end groups of PTMO a methanol was stripped off. At the end of the transesterification, the melting temperature of the reaction mixture was below 250°C, allowing a polycondensation in the melt. Firstly, NMP was distilled off at a low vacuum and then the pressure was reduced further to carry out the polycondensation. PBT–PTMO copolymers are known to melt phase during polymerization at certain polymer compositions [28]. Melt phasing will inhibit the formation of high molecular weight polymers. In Fig. 6 melt phasing of PBT–PTMO polycondensations as a function of the PTMO content and length is shown. In PBT–PTMO copolymers melt phasing is enhanced by decreasing the PTMO content and increasing the PTMO length. In these systems, decreasing the PTMO content while keeping the PTMO length constant results in an increase of the PBT segment length. Longer PBT segments melt phase at a lower concentration than short PBT segments. The T $\Phi$ T units are of uniform thickness and cannot become longer. During the polycondensation of T $\Phi$ T–PTMO copolymers a homogeneous melt was obtained at all compositions. Apparently in T $\Phi$ T–PTMO copolymers the PTMO content is always high enough to avoid melt phasing and consequently high molecular weight PTMO segments can be used without melt phasing to occur. To illustrate this, the points of T $\Phi$ T–PTMO are included in Fig. 6. The melt phasing region of T $\Phi$ T–PTMO probably lies at a somewhat different polymer composition compared to PBT–PTMO, indicated by the dotted line.

During the polycondensation of T $\Phi$ T–PTMO copolymers, the rest of the methanol was removed, the reaction equilibrium shifted to the right and high molecular weight polymers were obtained. As a relative measure of the molecular weight, the inherent viscosity is used ( $\eta_{inh}$ ) and inherent viscosities up to 2.8 dl/g were obtained. The polymers were gold-yellow, the typical aramid color. To get an

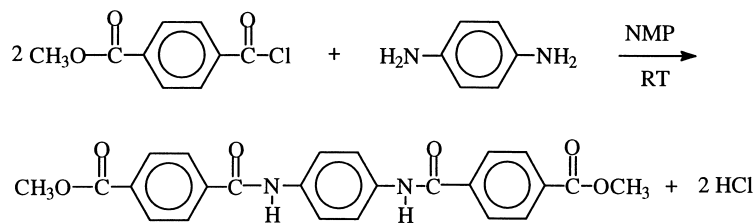


Fig. 4. Reaction scheme for the synthesis of TΦT-dimethyl from methyl(4-chlorocarbonyl)benzoate and *p*-phenylenediamine (route II).

impression of the molecular weight, GPC measurements in *m*-cresol were carried out on four batches of TΦT-PTMO<sub>2000</sub> with different inherent viscosities. The values for  $M_n$  are not absolute values, but relative to a polystyrene standard. The absolute values for  $M_n$  are probably lower due to differences in interaction of polymer with the elution solvent or swelling of the polymers in *m*-cresol. The relative values of  $M_n$  are given in Fig. 7 and they are plotted versus the inherent viscosity. In general, the  $M_n$  of a polymer in solution is related to the intrinsic viscosity according to the Mark–Houwink equation [29]

$$[\eta] = kM_n^a \quad (3)$$

If the concentration of the polymer solution approaches zero, the intrinsic viscosity equals the inherent viscosity. The inherent viscosity was measured at a concentration of 0.1 dl/g, low enough to make this assumption. According to Eq. (3), the values in Fig. 7 can be fitted with an exponential curve.

#### 3.4. Melt polymerization (route II)

A melt polymerization can be carried out using TΦT-didecanyl instead of TΦT-dimethyl. The melting temperature of TΦT-didecanyl is 271°C, still too high for melt polymerization. This problem was overcome by applying a short reactive extrusion step at 275°C to start the transesterification. The raw materials (catalyst solution included) were

mixed and extruded. The melting temperature of the extrudate was reduced just below 250°C and consequently the rest of the transesterification and the subsequent polycondensation could be carried out in a normal reaction vessel at 250°C. The inherent viscosities of the polymers synthesized according to this route ranged from 0.7 to 1.1 dl/g, suggesting reasonably high molecular weights. It seems to be easier, however, to obtain high molecular weight polymers via route I (solution/melt polymerization).

#### 3.5. Solvent free one pot polymerization of TΦT-PTMO copolymers (route III)

A possible way to synthesize TΦT-PTMO copolymers in one reactor would be by first esterifying the hydroxyl end groups of PTMO with terephthalic acid based compounds (I, phenyl terephthalate, terephthaloyl chloride or terephthalic acid end groups) providing compounds II with the corresponding end groups. In a second step, the end groups could be reacted with *p*-phenylenediamine or, in case of acid end groups also with 1,4-phenylenediisocyanate to form the polymer. The proposed reaction scheme is given in Fig. 8. To obtain uniform TΦT segments, no unreacted terephthalate molecules are allowed to be present after the first step. For the stoichiometry of the reaction, and thus final molecular weight of the polymer, all hydroxyl end groups should be converted into terephthalic based groups. The different possibilities are discussed in the following part.

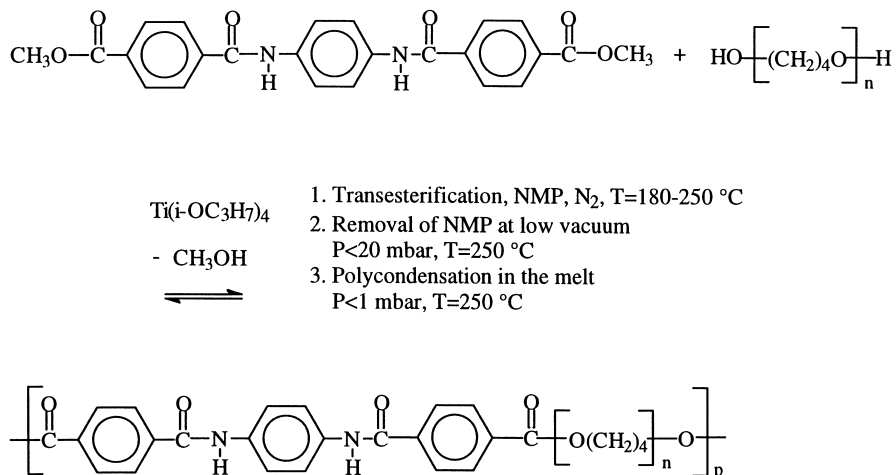


Fig. 5. Polymerization of TΦT-PTMO.

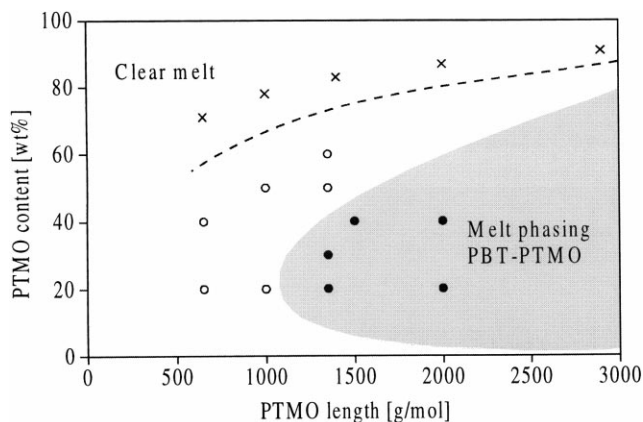


Fig. 6. Melt phasing in polycondensations as a function of PTMO content and length for (●, ○) PBT-PTMO copolymers [28] and (×) TΦT-PTMO. The melt phasing region of PBT-PTMO is indicated, the dotted line indicates the expected melt phasing transition of TΦT-PTMO copolymers.

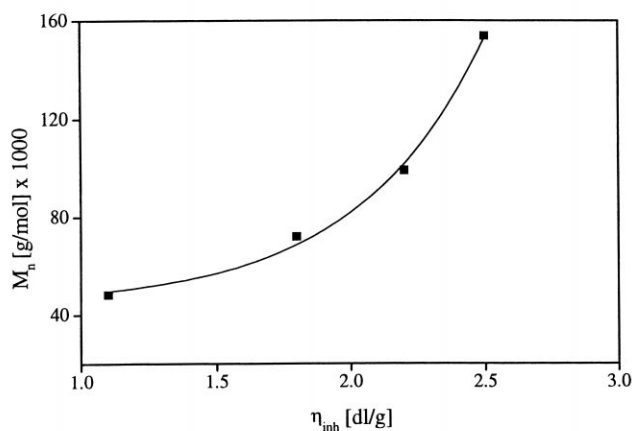
### 3.6. Starting from PTMO, diphenyl terephthalate and *p*-phenylenediamine

To obtain uniform hard segments, it is important to carry out the esterification to its completion, which is in general, difficult. Since phenol is a good leaving group, the esterification of PTMO with diphenyl terephthalate should proceed fast and therefore it might be possible to reach full conversion of the hydroxyl end groups into ester end groups. Diphenyl terephthalate was synthesized as described in Section 2. The melting temperature, as measured with DSC is 200°C. In a first attempt, 2 mol of diphenyl terephthalate were reacted with 1 mol of PTMO at 220°C in the melt, tetraisopropyl orthotitanate being used as the catalyst. <sup>1</sup>H NMR analysis of the product showed that still some unreacted diphenyl terephthalate was present and that part of the phenyl terephthalate end groups had reacted to form longer segments such as phenyl terephthalate-PTMO-terephthalate-PTMO-phenyl terephthalate. As

long as all the hydroxyl end groups are transformed into phenyl terephthalate end groups, the only side effect is the formation of these longer segments which is at the same time an effective way of increasing the average soft segment length. The soft segment length can be calculated from the <sup>1</sup>H NMR integrals and the amount of *p*-phenylenediamine needed can be adjusted. To avoid the presence of free diphenyl terephthalate, PTMO and diphenyl terephthalate were reacted in a molar ratio of 1:1.5. <sup>1</sup>H NMR analysis of the product showed the absence of diphenyl terephthalate and hydroxyl end groups in the product. The overall soft segment length was 4773 g/mol. A product like this could be used as the soft segment for the polymerization.

To polymerize diphenyl terephthalate with *p*-phenylenediamine without a catalyst to form the aromatic polyamide, a polymerization temperature of 325°C was reported [30]. For PTMO, the maximum allowable polymerization temperature is 250°C due to thermal degradation. By using sodium methanolate as a catalyst the polymerization temperature for the reaction between phenyl terephthalate end groups and *p*-phenylenediamine might be reduced. Bouma [31] showed that sodium methanolate is a very effective catalyst for these type of reactions. To check whether phenyl terephthalate groups react with *p*-phenylenediamine, one mole diphenyl terephthalate was reacted with two moles of *p*-phenylenediamine in the presence of sodium methanolate. The reaction temperature was 200°C and the reaction was carried out in a solution of NMP. The <sup>1</sup>H NMR spectrum with the peak assignment of the product is given in Fig. 9. The NMR spectrum shows that about 90% of the *p*-phenylenediamine has reacted with diphenyl terephthalate to form the diamide terephthalate. Hence it can be concluded that the reaction of *p*-phenylenediamine with diphenyl terephthalate in the presence of sodium methanolate as a catalyst is very effective.

The melting temperature of *p*-phenylenediamine is 145°C and thus a melt polymerization of *p*-phenylenediamine with phenyl terephthalate end-capped PTMO to form a



Molecular weight of TΦT-PTMO<sub>2000</sub> relative to Polystyrene standards

$\eta_{inh}$ [dl/g]	$M_n \times 1000$ [g/mol]
1.1	48.3
1.8	72.1
2.2	99.1
2.5	153.8

Fig. 7. Relative number average molecular weight of TΦT-PTMO<sub>2000</sub> versus inherent viscosity.



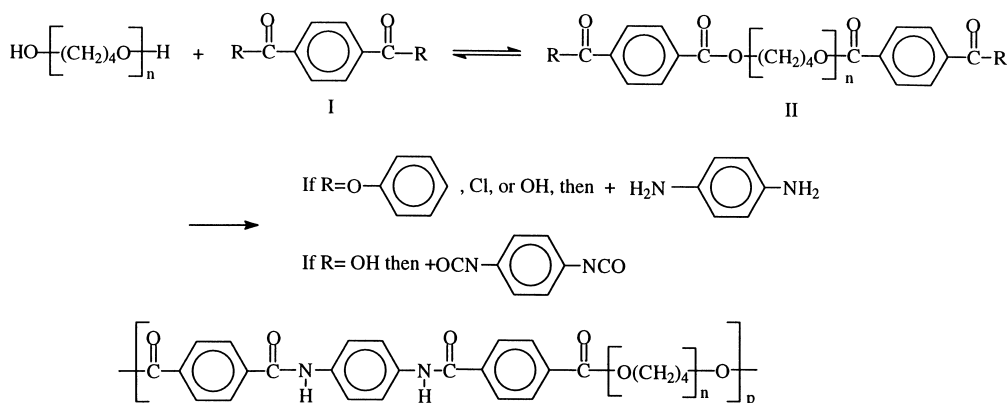


Fig. 8. Proposed reaction scheme for the polymerization of TΦT-PTMO copolymers from end-capped PTMO (II) and *p*-phenylenediamine, or *p*-phenylenediisocyanate.

TΦT-(PTMO/DPT) copolymer should be possible. *p*-Phenylenediamine is very likely to sublime and therefore a two-fold excess was used for the polymerization. The excess of *p*-phenylenediamine was stripped at the end by applying low pressure. The obtained polymer was a flexible, brown and transparent solid.  $^1\text{H}$  NMR analysis showed the typical TΦT peaks with the expected integrals. No phenyl terephthalate end-group peaks were visible, neither a peak from free *p*-phenylenediamine. The inherent ( $\eta_{\text{inh}}$ ) of the polymer was 0.82 dl/g. It was concluded that the TΦT-(PTMO<sub>1000</sub>/DPT)<sub>4773</sub> polymer was formed. This route seems to be a very promising way for a solvent free one-pot polymerization of TΦT-PTMO copolymers. If diphenyl terephthalate is replaced by dimethyl terephthalate, the same polymer may be obtained. The reaction between aromatic diamines and dimethyl terephthalate is more difficult [29] and yet high molecular weight polymers were not obtained with dimethyl terephthalate.

### 3.7. Reaction between terephthaloyl chloride and PTMO

The reaction between PTMO and terephthalate chloride in the melt was problematic. Under these conditions PTMO was found to thermally degrade.

### 3.8. Reaction between terephthalic acid and PTMO

Terephthalic acid does not dissolve in pure PTMO. The melting temperature of terephthalic acid is over 300°C, too high to allow a reaction in the melt. The reaction between terephthalic acid and PTMO in an NMP solution is slow and therefore a strong esterification catalyst is needed. Tetraisopropyl orthotitanate is such a strong catalyst [32], however, it forms a complex with terephthalic acid, the complex precipitates, thereby preventing any reaction. Other catalysts, such as zinc acetate, gave a very slow reaction, even after 24 h, no esterification had occurred.

To conclude, the route, starting from diphenyl terephthalate, PTMO and *p*-phenylenediamine seems to be the most promising for a solvent free one-pot polymerization. The polymers for studying the properties, however, were synthesized according to route I, the solution/melt polymerization starting with TΦT-dimethyl and PTMO. Via this route, well defined polymers with uniform TΦT segments and high molecular weights are obtained.

### 3.9. Polymer properties

TΦT-dimethyl was copolymerized with different amorphous segments. The structures and abbreviations of the

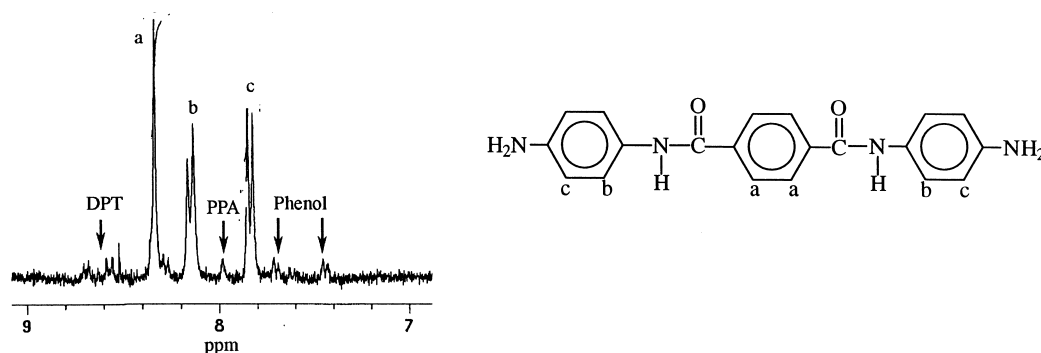


Fig. 9.  $^1\text{H}$  NMR spectrum with peak assignment of the reaction product of PPA and DPT.

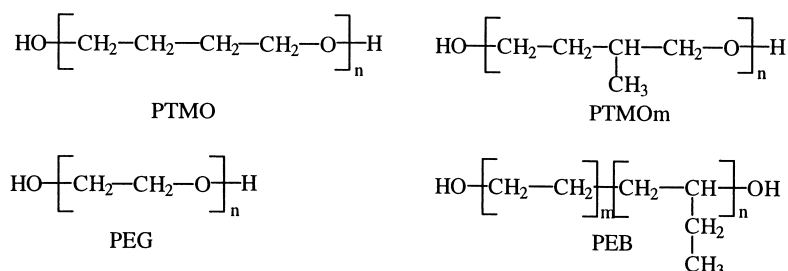


Fig. 10. Amorphous segments used in copolymers.

hydroxyl functionalized soft segments are given in Fig. 10. Besides the structure, the length of the soft segments in the polymers was varied. For this purpose a series of polymers with PTMO ranging from 650 to 2900 g/mol and polymers with PTMOm with a length of 1000 and 2000 were synthesized. The DSC and DMA results of the different polymers are given in Table 3. The inherent viscosities of the polymers with PTMO and PTMOm were high  $>1.1$  dl/g indicating that the molecular weights of the polymers were always high.

With DSC two melting and crystallization peaks were detected. The T $\Phi$ T segments form a crystalline phase ( $T_{m,h}$ ,  $T_{c,h}$ ) and PTMO segments longer than 1000 g/mol are known to crystallize just around room temperature [27] ( $T_{m,s}$ ,  $T_{c,s}$ ). The T $\Phi$ T melting and crystallization peaks were very weak and not visible at T $\Phi$ T contents below 20% (wt), suggesting that the difference in ordering between the molten T $\Phi$ T and the crystalline T $\Phi$ T segments is very small. The undercooling of the T $\Phi$ T segments ( $\Delta T_h = T_{m,h} - T_{c,h}$ ) is always lower than 30°C, indicating that the T $\Phi$ T segments crystallize fast. Poly(butylene terephthalate), which is considered as a fast crystallizing polymer has an undercooling of 36°C [33].

### 3.10. Variation of PTMO length

T $\Phi$ T–PTMO copolymers with a PTMO length ranging from 650 to 2900 g/mol were synthesized. Due to the uniform length of the hard segments, increasing the PTMO length, automatically results in a decrease of the hard segment content. In Fig. 11 the storage modulus ( $G'$ ) versus temperature is given for the T $\Phi$ T–PTMO copolymers. All the polymers possess a nearly temperature independent rubbery plateau and a very sharp flow transition. An explanation for this behavior is the formation of perfect crystalline lamellae from the uniform T $\Phi$ T segments. These lamellae of uniform thickness melt in a narrow temperature range. Close examination of the rubbery plateau reveals a slight increase of the rubbery modulus with temperature. This is typical for an elastomer and attributed to an increase of thermal motion of the chains with temperature making it harder to orient the elastomer [34]. The drop of the modulus at the  $T_g$  is very sharp, suggesting a well phase separated morphology. The polymers with PTMO<sub>2000</sub> and PTMO<sub>2900</sub> show a shoulder after the glass transition in the temperature range from  $-50$  to  $20^\circ\text{C}$ , caused by PTMO crystallization. Copolymers with PTMO lengths below

Table 3

Inherent viscosity, DSC and DMA results of T $\Phi$ T-copolymers (subscripts s refers to soft segments, h to T $\Phi$ T (hard) segment)

$M_s$ (g/mol)	$\eta_{inh}$ (dl/g)	$T_{m,s}$ (°C)	$\Delta H_{m,s}$ (J/g)	$T_{c,s}$ (°C)	$\Delta H_{c,s}$ (J/g)	$T_{m,h}$ (°C)	$\Delta H_{m,h}$ (J/g)	$T_{c,h}$ (°C)	$\Delta T_h$ (°C)	$T_g$ (°C)	$T_{fl}$ (°C)	$G'(25^\circ\text{C})$ (MPa)
<i>PTMO</i>												
650	1.40	–	–	–	–	266	12	238	28	–58	247	118
1000	1.57	–	–	–	–	222	10	203	19	–69	216	44
1400	1.92	–8	12	–46	–6	–	–	–	–	–70	198	15
2000	2.50	0	17	–39	–13	–	–	–	–	–65	191	9
2900	2.54	9	30	–31	–22	–	–	–	–	–70	170	6
<i>PTMOm</i>												
1000	1.10	–	–	–	–	259	9	234	25	–75	251	49
2000	2.38	–20	11	–	–	–	–	–	–	–75	193	10
<i>PEG</i>												
1000	0.73	–	–	–	–	–	–	–	–	–45	150	28
<i>PEB</i>												
3300	0.25 <sup>a</sup>	–	–	–	–	–	–	–	–	–60	120	2

<sup>a</sup> Measured in chloroform, 0.1 g/dl, 25°C.

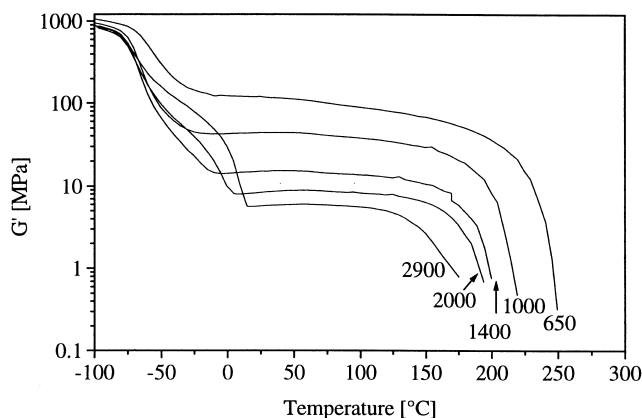


Fig. 11. Storage modulus ( $G'$ ) versus temperature for T $\Phi$ T-PTMO copolymers.

1000 g/mol have a two phase morphology: a T $\Phi$ T crystalline phase and a PTMO amorphous phase. Copolymers with PTMO lengths of 2000 g/mol and longer possess a three phase morphology: a crystalline T $\Phi$ T phase, a PTMO crystalline phase and a PTMO amorphous phase.

The flow temperature, defined as the temperature where the shear storage modulus reaches 1 MPa indicates the onset of melting and was therefore used as a measure of the melting temperature of the copolymers. As expected,  $T_{fl}$  was always a little lower than  $T_{m,h}$  measured with DSC. The  $T_g$ ,  $T_{fl}$ , and  $T_m$  of the PTMO phase are plotted versus the PTMO length in Fig. 12. As is clearly visible in this figure, the  $T_g$  is nearly independent of the PTMO length and thus also independent of the T $\Phi$ T content, suggesting that nearly all the T $\Phi$ T segments are in the crystalline phase. If there would be T $\Phi$ T segments present in the amorphous phase, the  $T_g$  would increase since rigid segments in the amorphous PTMO phase increases the  $T_g$ . It might be possible that a low concentration of T $\Phi$ T phase separates in a separate amorphous phase, however, a second  $T_g$  belonging to such a phase was not detected. The melting temperature of the PTMO crystalline phase appears at a PTMO length of 1400 g/mol and increases with the PTMO length. Longer PTMO segments have an improved long range order, facilitating the formation of larger crystals. Generally, the melting temperature of a polymer increases with the crystalline size (lamellar size) [35]. Table 3 shows an increase of the melting enthalpy with the PTMO length. Apparently, not only the crystalline size but also the crystallinity of the PTMO phase increases with the PTMO length. This is obvious since the PTMO content in the polymers increases with PTMO length.

The flow temperature decreases with increasing PTMO length. Normally for segmented copolymers, the decrease of the hard segment melting temperature upon copolymerization with a soft segment is explained by the solvent effect proposed by Flory [11] (Eq. (4))

$$\frac{1}{T_m} - \frac{1}{T_m^0} = -\left(\frac{R}{\Delta H_f}\right) \ln X_A [^{\circ}\text{K}^{-1}] \quad (4)$$

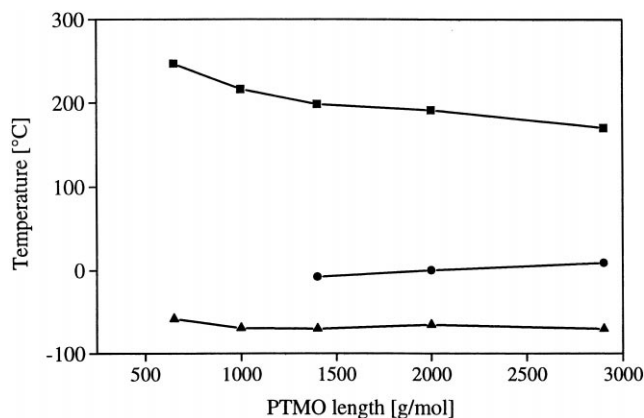


Fig. 12. Thermal transitions of T $\Phi$ T-PTMO segmented copolymers versus PTMO length (■— $T_{fl}$ , ●— $T_{m,PTMO}$ , ▲— $T_g$ ).

where  $T_m$  is the melting temperature of the copolymer,  $T_m^0$  the melting temperature of the homopolymer,  $X_A$  the molar fraction of crystallizable units in the copolymer,  $\Delta H_f$  the latent heat of fusion of the homopolymer, and  $R$  the gas constant. This equation is based on the assumption that the solution is ideal and that the enthalpy and entropy of melting are temperature independent. According to Eq. (4) differences in the melting temperature should then solely be ascribed to differences in  $X_A$ , the molar fraction of crystalline T $\Phi$ T units. Since no increase of the  $T_g$  with increasing T $\Phi$ T content was observed and no separate T $\Phi$ T glass transition was detected, the T $\Phi$ T crystallinity is assumed to be 100% and therefore the T $\Phi$ T content is used to calculate  $X_A$ . According to the theory of Flory, the molar volumes of the crystallizable and non-crystallizable units should be equal. The molar volume of a crystalline T $\Phi$ T unit is 2.9 times the molar volume of an amorphous PTMO repeat unit [36].  $X_A$  was then calculated with Eq. (5) in which  $n$  is the number of  $-(\text{CH}_2)_4\text{O}-$  repeat units in a PTMO segment

$$X_A = \frac{2.9}{2.9 + n} [-] \quad (5)$$

In Fig. 13, the values for the T $\Phi$ T-PTMO, T4T-PTMO (1,4-butanediamine based) and T2T-PTMO (1,2-ethanediamine based) copolymers are fitted in Eq. (4). A straight line can be fitted through the points, suggesting that Eq. (4) can be used to describe the melting point depression. The intercept with the y-axis of the fitted line corresponds well with the melting point of T $\Phi$ T-dimethyl; a  $T_{fl}^0$  of 360°C was found compared to a  $T_m$  of 371°C for T $\Phi$ T-dimethyl. The same procedure was applied to T4T-PTMO and T2T-PTMO copolymers, and also for these polymers straight lines can be fitted to the points and the calculated  $T_{fl}^0$ 's correspond well with the bisesterdiamides;  $T_{fl}^0 = 268^\circ\text{C}$  (T4T-dimethyl;  $T_m = 265^\circ\text{C}$ ) and  $T_{fl}^0 = 329^\circ\text{C}$  (T2T-dimethyl;  $T_m = 310^\circ\text{C}$ ).

Usually TPE's from segmented copolymers can be made with a range of rubbery moduli by changing the hard segment content [1]. Fig. 14 shows a linear increase of the

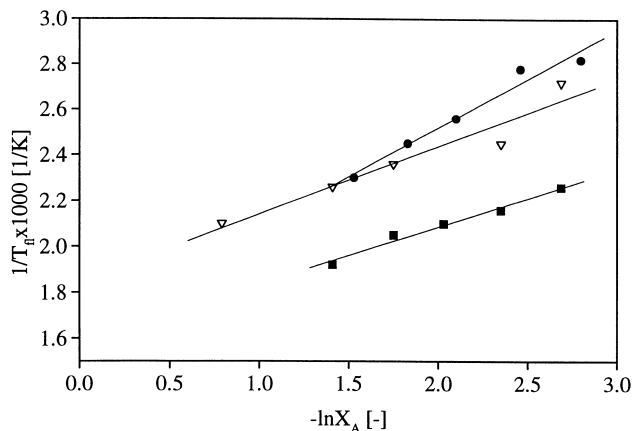


Fig. 13.  $1/T_g$  versus  $-\ln X_A$  for (■) TΦT-PTMO, (▽) T4T-PTMO [10] and (●) T2T-PTMO [37] copolymers.

logarithm of the shear rubbery modulus ( $G'$ ) with the aramid content. The increase can be explained by an increase in crystallinity and thus increase in physical crosslink density, making the polymer stiffer. TPE's with a low modulus are interesting since they are flexible and elastic. The modulus of TΦT-PTMO copolymers can reach lower values combined with a higher melting temperature than those of commercial poly(butylene terephthalate)-polyether segmented copolymers, for instance arnitel EM400 has a rubbery modulus of 18 MPa with a flow temperature of 184°C, compared to a rubbery modulus of 9 MPa and a flow temperature of 191°C for TΦT-PTMO<sub>2000</sub>. A low modulus can be obtained by using a low TΦT concentration and thus long PTMO segments. The disadvantage of long PTMO segments is that they crystallize around room temperature. In Fig. 11 this PTMO crystallization is visible as a shoulder in the drop of the modulus near the  $T_g$ . The rubbery plateau starts at a higher temperature and hence the low temperature flexibility is reduced.

### 3.11. Different types of soft segments

Besides PTMO soft segments, also polymers with PTMOm, PEG<sub>1000</sub> and PEB<sub>3000</sub> soft segments were synthesized (Table 3). The polymerization temperature of 250°C is rather high for PEG<sub>1000</sub>, PEG already starts to thermally degrade at 100°C. The relatively low inherent viscosity ( $\eta_{inh} = 0.73$  dl/g), indicating a low molecular weight, is probably caused by thermal degradation during synthesis. With DSC no melting and crystallization transitions were observed for TΦT-PEG<sub>1000</sub>. In the TΦT-PTMO copolymers, hard segment melting and crystallization peaks were visible at TΦT contents above 22 wt%, suggesting that TΦT-PEG<sub>1000</sub> is less crystalline than TΦT-PTMO<sub>1000</sub>, since for both polymers the TΦT content is 22 wt%. PEB segments phase separate from TΦT during synthesis, therefore it was not possible to obtain high molecular weight polymers. To compare the different soft segments the

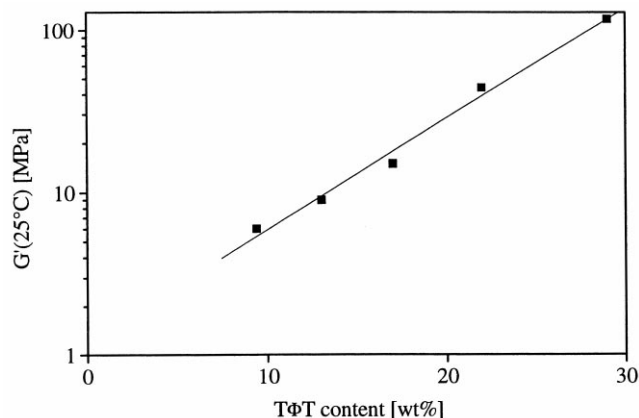


Fig. 14. Logarithm of the shear rubbery modulus ( $G'$ ) versus TΦT content in TΦT-PTMO copolymers.

storage ( $G'$ ) and loss modulus ( $G''$ ) are given versus temperature in Fig. 15a and b, respectively. The  $T_g$  of the polymers containing PTMOm is somewhat lower than of the polymers containing PTMO (−75 and −65°C, respectively). The methyl-side groups of the PTMOm chains lower the  $T_g$ . The flow temperature of TΦT-PTMO<sub>1000m</sub> is higher than of TΦT-PTMO<sub>1000</sub>, mainly because PTMO<sub>1000m</sub>

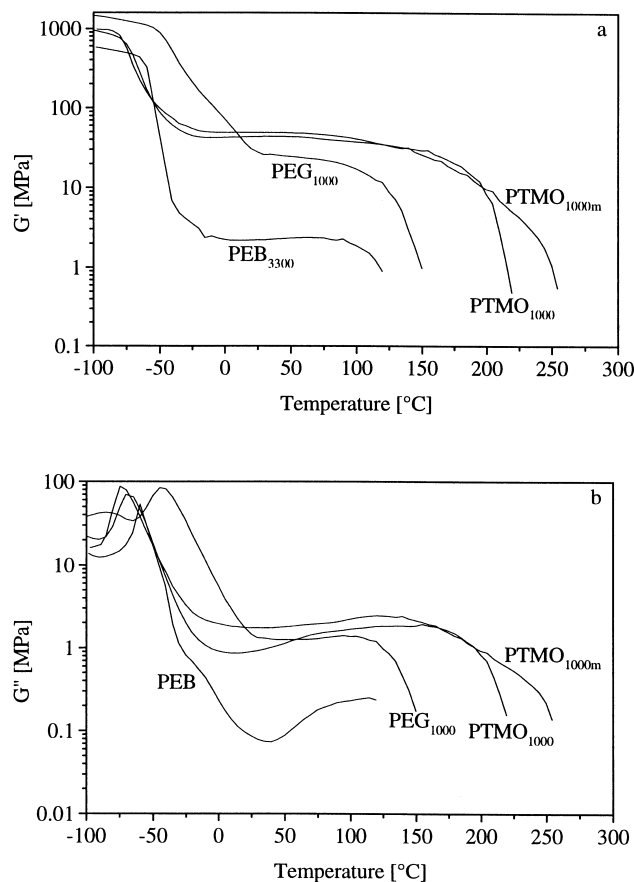


Fig. 15. (a) Storage ( $G'$ ) and (b) loss ( $G''$ ) modulus of TΦT-diol segmented copolymers.

Table 4

Results of water absorption of T $\Phi$ T–PTMO<sub>1000</sub>, T $\Phi$ T–PTMO<sub>1000m</sub>, T $\Phi$ T–PEG<sub>1000</sub>, and Arnitel EL550 (commercial segmented copolymer: PBT–PTMO), for seven days at RT, 100% RH

Polymer	Water absorption (wt%)
T $\Phi$ T–PTMO <sub>1000</sub>	1.0
T $\Phi$ T–PTMO <sub>1000m</sub>	0.9
T $\Phi$ T–PEG <sub>1000</sub>	80.5
Arnitel EL550	0.9

is shorter than PTMO<sub>1000</sub> resulting in a smaller solvent effect. PEG<sub>1000</sub> segments have a  $T_g$  of  $-55^\circ\text{C}$  [38]. The  $T_g$  of T $\Phi$ T–PEG<sub>1000</sub> is  $-45^\circ\text{C}$ , which is higher than the  $T_g$  of PEG<sub>1000</sub> segments itself and is attributed to the presence of the T $\Phi$ T physical crosslinks. The peak of the loss modulus ( $G''$ ) at the  $T_g$  of T $\Phi$ T–PEG<sub>1000</sub> is broad compared to the other polymers suggesting that the phase separation of the T $\Phi$ T segments in PEG is not as good as in PTMO, PTMOm and PEB. The rubbery modulus ( $G'$ ) of T $\Phi$ T–PEG<sub>1000</sub> is lower than of T $\Phi$ T–PTMO<sub>1000</sub> indicating that the T $\Phi$ T crystallinity in PEG is lower than in PTMO or that the modulus of pure PEG is lower than of pure PTMO. The flow temperature of T $\Phi$ T–PEG<sub>1000</sub> is also lower compared to T $\Phi$ T–PTMO<sub>1000</sub>. This is probably caused by a lower T $\Phi$ T crystallinity in T $\Phi$ T–PEG copolymers than in T $\Phi$ T–PTMO copolymers leading to a smaller solvent effect. The glass transition of T $\Phi$ T–PEB<sub>3300</sub> is very sharp indicating a very good phase separation. During synthesis, phase separation already occurred and taking into account the low inherent viscosity, it is very likely that not all of the T $\Phi$ T-dimethyl has reacted. The very low rubbery modulus of only 2 MPa might also be caused by the lower modulus of poly(ethylene/polybutylene) itself compared to PTMO and PEG. PEB segments can give polymers with very interesting properties, the problem, however, is the phase separation during synthesis which limits the molecular weight. Higher molecular weights may be obtained if the PEB segments are first modified with terephthalic acid end groups, followed by a reaction with aromatic diamines or aromatic diisocyanates as discussed before.

### 3.12. Water absorption

Polyamides are known for their high water absorption. Polymers with bisesterdiamides are highly crystalline. In general, the crystalline phase is inaccessible for water and water is absorbed by the amorphous phase. Poly(oxyethyleneglycol) is very hydrophilic and consequently absorbs water easily [37]. This feature could make T $\Phi$ T–PEG copolymers interesting for TPE's used in applications to absorb water, for instance, semi-permeable cloths for rain protection and diapers. In Table 4, the water absorption of T $\Phi$ T copolymers with different polyether segments is presented. As a comparison the water absorption of a commercial segmented PBT–PTMO copolymer (Arnitel EL550) is

given. The water absorption of the PTMO containing polymers is very low, only 1%. The PTMO phase does not absorb water easily. As expected, the water absorption of T $\Phi$ T–PEG<sub>1000</sub> is high: 80.5%. If the PEG segment length is increased and thus the diamide content decreased, even higher water absorption values are expected. By mixing PTMO and PEG, the water uptake can probably be adjusted to a desired value.

## 4. Conclusion

Segmented copolymers with T $\Phi$ T hard segments and PTMO, PTMOm, PEG or PEB soft segments were synthesized. Well defined polymers with uniform T $\Phi$ T segments and high molecular weights were obtained by a solution/melt polymerization of T $\Phi$ T-dimethyl with hydroxyl functionalized PTMO. T $\Phi$ T-dimethyl was synthesized from terephthaloyl chloride, *p*-phenylenediamine and methanol (route I) or from methyl(4-chlorocarbonyl)benzoate and *p*-phenylenediamine (route II). Following route II, both the yield and purity were high. The melting temperature of T $\Phi$ T-dimethyl is so high ( $371^\circ\text{C}$ ) that a solvent (NMP) is needed for the polymerization. The polymerization consists of a transesterification in solution, followed by a polycondensation in the melt. No melt phasing occurs during the polycondensation, since the T $\Phi$ T content is always low enough. Replacing T $\Phi$ T-dimethyl with T $\Phi$ T-didecanyl allows a complete melt polymerization since the melting temperature of T $\Phi$ T-didecanyl is low enough:  $272^\circ\text{C}$ . A solvent free one-pot polymerization is possible by first reacting PTMO with an excess of diphenyl terephthalate. Subsequently adding *p*-phenylenediamine in the presence of sodium methanolate as the catalyst yields T $\Phi$ T–(PTMO/DPT) copolymers.

T $\Phi$ T–PTMO copolymers with PTMO lengths ranging from 650 to 2900 g/mol were synthesized. They possess a well phase separated morphology. Below PTMO lengths of 1400 g/mol, the polymers consist of two phases: a crystalline T $\Phi$ T phase and an amorphous PTMO phase. Polymers with PTMO segments longer than 1400 g/mol consist of three phases: a crystalline T $\Phi$ T phase, an amorphous PTMO phase and a crystalline PTMO phase. The glass transition temperature is sharp at  $-65^\circ\text{C}$  and almost independent of the PTMO length, suggesting that in the amorphous polyether phase a low concentration of T $\Phi$ T segments is present. The rubbery plateau is temperature independent and the flow transition is very sharp. This is attributed to the uniform T $\Phi$ T segment forming perfect crystals that melt in a narrow temperature range. The logarithm of the rubbery modulus increases linearly with the aramid content (6–118 MPa, 9–29 wt% T $\Phi$ T), due to an increase in crystallinity and consequently increase in physical crosslink density. Compared to commercial segmented copolyetheresters (PBT–PTMO) softer material can be obtained with a comparable melting temperature. The low

undercooling ( $\Delta T_h = T_{m,h} - T_{c,h} < 30^\circ\text{C}$ ) of the T $\Phi$ T segments, measured with DSC, suggests fast crystallization of the T $\Phi$ T segments even at very low concentrations (<15 wt%). The decrease of the flow temperature (248–170°C) with increasing soft segment length (650–2900 g/mol) can be explained by the solvent effect. The properties of polymers with PTMO and PTMOM are comparable. Polymers with PTMOM have a lower glass transition temperature ( $-75^\circ\text{C}$ ) and thus an improved low temperature flexibility.

With PEG it was not easy to obtain high molecular weight polymers due to thermal degradation of PEG during synthesis at 250°C. T $\Phi$ T-PEG<sub>1000</sub> has a  $T_g$  of  $-45^\circ\text{C}$  and a flow temperature of 150°C. The rubbery plateau is somewhat more temperature dependent than of the other polymers. These results suggest that the T $\Phi$ T crystallinity in this polymer is lower compared to the other polymers. The water uptake of this polymer was high, 80.5% due to the hydrophilic PEG segments.

PEB<sub>3300</sub> soft segments yield polymers with a very good phase separation: the  $T_g$  is extremely sharp, the rubbery plateau is temperature independent and the flow temperature is also sharp. The rubbery modulus is very low, only 2 MPa. The problem of this polymer, however, is the phase separation that already occurs during synthesis, prohibiting the formation of high molecular weight polymers.

## References

- [1] Holden G, Legge NR, Quirk R, Schroeder HE. Thermoplastic elastomers. 2nd ed. Munich: Hanser, 1996.
- [2] Cella RJJ. J Polym Sci 1973;42:727–40.
- [3] Harrell LL. Macromolecules 1969;2(6):607–12.
- [4] Ng HN, Allegrazza AE, Seymour RW, Cooper SL. Polymer 1973;14:255–61.
- [5] Eisenbach CD, Baumgarthner M, Gunter G. In: Lal L, Mark JE, editors. Advances in elastomer and rubber elasticity, Proc Symposium, vol. 51. New York: Plenum, 1985.
- [6] Miller JA, Shaow BL, Hwang KKS, Wu KS, Gibson PE, Cooper SL. Macromolecules 1985;18(1):32–44.
- [7] Kirikihira I, Yakakawa H, Kubo Y. EP Patent 0 608 976 A1, Tosoh Corporation, Japan 1994.
- [8] Hirt P, Herlinger H. Die Angew Makromol Chem 1974;40/41(601):71–88.
- [9] Gaymans RJ, de Haan JL. Polymer 1993;34(20):4360–4.
- [10] Van Hutten PF, Mangnus RM, Gaymanus RJ. Polymer 1993;34(20):4193–201.
- [11] Flory PJ. Trans Faraday Soc 1955;51:848–57.
- [12] Sorta E, Della Fortuna G. Polymer 1980;21:728–32.
- [13] Greene RN, Figuly GD. US Patent 4, 731, 435, E.I. Du Pont de Nemours and Company, USA 1988.
- [14] Ishimaru, Toshiaki, Nishizawa, Hiroshi, Kitaibaraki, Osada, Yuichi, D.E., Patent 29 00 932, Hitachi Chemical Co., Ltd, Japan 1979.
- [15] Mangnus R. Terephthalamide–PTMO segmented copolymers with a uniform block length, University of Twente:twaiio report 1992.
- [16] Den Breejen C. Gesegmenteerde blockcopolymeren gebaseerd op uniforme aramide blokken, University of Twente:twaiio report, 1994.
- [17] Coope JL. US Patent 5,268,003, Lever Borthers Company, Division of Conopco Inc., USA 1993.
- [18] Coope JL. US Patent 5,397,501, Lever Borthers Company, Division of Conopco Inc., USA 1995.
- [19] Chang S, Chang F, Tsai H. Polym Eng Sci 1995;35(2):190–4.
- [20] Greene RN. US Patent 5,116,937, E.I. Du Pont de Nemours and Company, USA 1992.
- [21] Imai Y, Kajiyama M, Ogata S, Kakimoto M. Polym J 1985;17(4):1173–8.
- [22] Ueda M, Sato, Imai Y. J Polym Sci 1979;17:783–7.
- [23] Chen AT, Farrissey J, Nelb G. US Patent 4,129,715, The Upjohn Company, USA 1978.
- [24] Chen AT, Onder K. US Patent 4,649,180, The Dow Chemical Company, USA 1987.
- [25] Jeong HM, Moon SW, Jho JY, Ahn TO. Polymer 1998;39(2):459–65.
- [26] Schotman AHM, Weber TJM, Mijs WJ. Macromol Chem Phys 1999;200(3):635–41.
- [27] Dreyfuss P, Drefuss MP, Pruckmayr G. In: Mark, Bikales, Overberger, Menges, editors. Encyclopedia of polymer science and engineering, vol. 16. New York: Wiley, 1989. p. 649–76.
- [28] Adams RK, Hoeschele GK. In: Legge NR, Holden G, Schroeder HE, editors. Thermoplastic elastomers, 1 ed. Munich: Hanser, 1987 (chap. 8).
- [29] Hiemenz PC. Polymer chemistry, the basic concepts. New York: Marcel Dekker, 1984 (chap. 9).
- [30] Vollbracht L. In: Eastmond GC, Ledwith A, Russo S, Sigwalt P, editors. Comprehensive polymer science, vol. 5. Oxford: Pergamon, 1989 (chap. 22).
- [31] Bouma K, Lohmeijer JHGM, Gaymans RJ. Polymer 2000;41:2719–25.
- [32] Pilati F. In: Allen G, Bevington JC, editors. Comprehensive polymer science, vol. 5. Oxford: Pergamon, 1989. p. 280.
- [33] Van Bennekom ACM, Gaymans RJ. Polymer 1997;38(3):657–66.
- [34] Cowie JMG. Polymers: chemistry and physics of modern materials. Glasgow: Blackie Academic, 1991 (chap. 14).
- [35] Hiemenz PC. Polymer chemistry, the basic concepts. New York: Marcel Dekker, 1984 (chap. 4).
- [36] Van Krevelen DW. Properties of polymers. Amsterdam: Elsevier, 1976.
- [37] Bouma K, Wester G, Gaymans RJ. J Appl Polym Sci (submitted).
- [38] Braun BB, DeLong DJ. In: Mark HF, Othmer DF, Overberge EG, Seaborg GT, editors. Kirk Othmer encyclopedia of chemical technology, vol. 18. New York: Wiley, 1982. p. 617.